J. Fluid Mech. (2003), *vol.* 474, *pp.* 95–115.
DOI: 10.1017/S0022112002002495 Printed in the United Kingdom

Effects of solute mass transfer on the stability of capillary jets

By G. O. COLLANTES[1], E. YARIV[2] AND I. FRANKEL[1]

[1]Faculty of Aerospace Engineering, Technion – IIT, Haifa 32000, Israel

[2]Faculty of Mathematics, Technion – IIT, Haifa 32000, Israel

(Received 8 March 1999 and in revised form 10 July 2002)

The effects of mass transfer (e.g. via evaporation) of surface-active solutes on the hydrodynamic stability of capillary liquid jets are studied. A linear temporal stability analysis is carried out yielding evolution equations for systems satisfying general non-linear kinetic adsorption relations and accompanying surface constitutive equations. The discussion of the instability mechanism associated with the Marangoni effect clarifies that solute transfer into the jet is destabilizing whereas transfer in the opposite direction reduces instability. The general analysis is illustrated by a system satisfying Langmuir-type kinetic relations. Contrary to a clean system (i.e. in the absence of surfactants), reduced jet viscosity may lead to a substantial reduction in perturbation growth. Furthermore, the Marangoni effect gives rise to an overstability mechanism whereby perturbations whose dimensionless wavenumbers exceed unity grow with time through oscillations of increasing amplitude. The common diffusion-control approximation constitutes an upper bound which substantially overestimates the actual growth of perturbations. Considering solutes belonging to the homologous series of normal alcohols in water–air systems, the intermediate cases (e.g. hexanol–water–air which is 'mixed-control') are the most susceptible to Marangoni instability.

1. Introduction

Stability and breakup of capillary jets are important in a wide variety of engineering applications (e.g. fuel injection, ink-jet printing, fibre spinning, etc.). Consequently, this problem has been extensively investigated. The numerous extensions of the pioneering analysis of Rayleigh (1878) include the incorporation of such additional effects as the jet viscosity, dynamics of the surrounding medium, non-Newtonian rheology, and non-uniformity of material properties ('compound' jets); the analysis of spatial (as opposed to temporal) convective and absolute stability, the study of the occurrence of satellite droplets and the recent modelling of the breakup phase by means of appropriate singular similarity solutions.

We here focus on the effect on jet stability of the transfer of adsorbing solutes across the jet surface. The presence of such solutes, which is often inevitable in engineering systems, modifies the local dynamic properties of the jet surface (e.g. reducing the surface tension). Non-uniformity of the surface adsorbed concentration results in surface tractions acting to induce bulk fluid motions which, in turn, may further enhance the surface concentration non-uniformity. The main goal of the present contribution is to clarify the influence of solute mass transfer on this Marangoni effect.

In the absence of solute mass transfer between the jet and its surrounding atmosphere Anshus (1973) found that the presence of surfactants had only a relatively minor stabilizing effect. However, abundant empirical evidence (cf. Skelland & Walker 1989, as well as references therein) indicates that solute mass transfer substantially affects jet stability, which motivates the present analysis.

Berg and coworkers (Burkholder & Berg 1974; Coyle, Berg & Niwa 1981) have addressed this problem. Their analysis, however, made use of the *ad hoc* assumption that the reference state could be characterized by a uniform and steady radial gradient of solute concentration. Tarr & Berg (1980) attempted to refine the model by assuming a steady boundary-layer-like reference distribution consisting of a linear variation in an annular domain adjacent to the jet surface and a constant concentration within the core. None of these distributions corresponds to a state of equilibrium between the jet and the ambient medium. They are therefore inconsistent with the steadiness assumption underlying these stability analyses. (Indeed, actual reference distributions are highly transient and nonlinear, see figure 1.) Thus, obvious difficulties arise in attempting to estimate the parameters incorporating the assumed constant gradient, which render questionable comparison of results of the above analyses with experimental data pertaining to any specific physical case.

No such *ad hoc* assumptions are made in the present contribution. Thus, rather than postulating a reference state, we first calculate (essentially following MacLeod & Radke 1994) the evolution of the reference concentration distribution. Stability of the resulting inherently unsteady reference state is subsequently analysed via the formulation and solution of an appropriate initial-value problem for the evolution of perturbations (rather than the standard eigenvalue problem). Use of this method has previously been made in the stability analysis of unsteady flows† associated with growing or collapsing bubbles (Prosperetti 1977) and elongating capillary jets (Frankel & Weihs 1987). Moreover, the entire analysis leading to the evolution equations applies to arbitrary nonlinear material laws and is not restricted to the commonly assumed equilibrium adsorption (which, in fact, is inadequate for the present problem, see § 5).

The rest of this contribution is organized as follows: In the next section we formulate and solve the problem for the reference-state concentration distribution. Subsequently, in § 3 we obtain the linear equations governing the evolution of small perturbations. In § 4 we discuss the various physical mechanisms at work, focusing on the coupling between the jet-surface displacement and the surface-excess concentration perturbation. Explicit results are presented for a system satisfying Langmuir-type kinetic relations. In § 5 we further comment on the consequences of the initial lack of equilibrium, the analogy between the present mechanism of instability and surface-tension-induced cellular convection as well as the (in)applicability of the diffusion-control approximation to the present problem. Finally, calculation of the vorticity distribution and estimates of the kinetic parameters are outlined in the Appendices.

† The initial-value approach has also been applied to the analysis of the stability of steady capillary jets as well as a number of other genuinely time-independent problems (see Berger 1988, and references cited therein). Apparently, the standard normal-mode method could (at least formally) be applied to these steady problems. However, the occurrence of continuous eigenvalue spectra makes the use of the initial-value approach essential in obtaining system response at physically relevant times.

2. Evolution of the reference state

The reference state of the present problem is characterized in terms of $C^{(0)}(r,t)$, the bulk concentration distribution within the jet, $\Gamma^{(0)}(t)$, the surface-excess concentration and $C_s^{(0)}(t)$, the bulk solute concentration at the outer surface of the jet (i.e. within the surrounding atmosphere). While the problem governing the evolution of these concentrations could in principle be formulated and solved for arbitrary initial conditions, it seems most plausible to assume that, for a liquid jet issuing from an orifice, the bulk concentrations within both phases are initially uniform whereas the 'freshly formed' free surface is initially clean, i.e.

$$C^{(0)}(r,0) = C_0, \quad C_s^{(0)}(0) = C_\infty, \quad \Gamma^{(0)}(0) = 0. \tag{2.1a–c}$$

Obviously, these represent a non-equilibrium initial state. Adopting a frame of reference moving with the presumed uniform axial liquid velocity, $C^{(0)}(r,t)$ satisfies the diffusion equation

$$\frac{\partial C^{(0)}}{\partial t} = D\left(\frac{\partial^2 C^{(0)}}{\partial r^2} + \frac{1}{r}\frac{\partial C^{(0)}}{\partial r}\right) \quad \text{for} \quad 0 < r < a \tag{2.2}$$

together with the boundary condition

$$\frac{\partial C^{(0)}}{\partial r} = 0 \quad \text{at} \quad r = 0. \tag{2.3}$$

Evolution of $C^{(0)}(r,t)$, $C_s^{(0)}(t)$ and $\Gamma^{(0)}(t)$ is coupled through the surface mass balance

$$\frac{\mathrm{d}\Gamma^{(0)}}{\mathrm{d}t} = -D\frac{\partial C^{(0)}}{\partial r} - E(C_s^{(0)} - C_\infty) \quad \text{at} \quad r = a \tag{2.4}$$

supplemented by the kinetic relations

$$\Phi_l(C^{(0)}, \Gamma^{(0)}) = -D\frac{\partial C^{(0)}}{\partial r} \quad \text{at} \quad r = a \tag{2.5a}$$

and

$$\Phi_g(C_s^{(0)}, \Gamma^{(0)}) = -E(C_s^{(0)} - C_\infty) \quad \text{at} \quad r = a. \tag{2.5b}$$

In the above D denotes solute diffusivity and a is the radius of the unperturbed jet. The surface mass balance (2.4) equates the rate of adsorption to the difference between the diffusive flux towards the jet surface and the rate of mass transfer to the surrounding atmosphere. The latter flux is represented in the usual manner (cf. Hansen 1960; Crank 1975) by the radiation-type term characterized by the (presumed constant) mass-transfer rate coefficient E. In (2.5) Φ_l and Φ_g express the respective kinetic rates of adsorption from each phase in terms of instantaneous values of the surface-excess and appropriate subsurface concentrations. Explicit functional forms will be specified later on (cf. (4.1)).

We normalize the radial coordinate by the jet radius a, the bulk concentrations by the sum $\overline{C} = C_0 + C_\infty$ of the initial concentrations, the surface-excess concentration by the saturation value Γ_m and the kinetic rate expressions Φ_l and Φ_g by $\overline{C}K_l$ and $\overline{C}K_g$, respectively, wherein K_l and K_g are rate constants having the dimensions of length per unit time. With a view to subsequent stability analysis we choose to describe the evolution of the reference state on the capillary time scale $T_c = (\rho a^3/\sigma_0)^{1/2}$ in which ρ is the jet density and σ_0 is the value of the surface-tension coefficient corresponding to a clean surface. Since only dimensionless variables appear in the following we retain

for these new variables the same notation originally introduced for their dimensional counterparts.

Applying the foregoing normalization we obtain from (2.2) a dimensionless diffusion equation whose right-hand side is multiplied by the parameter

$$\epsilon = \frac{DT_c}{a^2}. \tag{2.6}$$

For typical values (cf. Appendix B) $\epsilon \approx 10^{-6}$. Subsequent analysis is facilitated by assuming that is ϵ asymptotically small. The 'outer' limit $\epsilon \to 0$ when $1 - r \sim O(1)$ yields† $C^{(0)}(r,t) = C_0$ which satisfies the dimensionless counterparts of (2.1*a*), (2.2) and (2.3) but cannot, in general, satisfy the boundary conditions (2.4) and (2.5) on the jet surface. We thus consider the 'inner' limit in terms of the variable x defined by

$$1 - r = \epsilon^{1/2} x. \tag{2.7}$$

To leading order in ϵ (2.1)–(2.5) yield in this limit

$$\frac{\partial C^{(0)}}{\partial t} = \frac{\partial^2 C^{(0)}}{\partial x^2} \quad \text{for} \quad 0 < x < \infty, \tag{2.8}$$

$$\frac{\mathrm{d}\Gamma^{(0)}}{\mathrm{d}t} = \frac{(DT_c)^{1/2}\overline{C}}{\Gamma_m}\frac{\partial C^{(0)}}{\partial x} + \frac{ET_c\overline{C}}{\Gamma_m}(C_\infty - C_s^{(0)}) \quad \text{at} \quad x = 0, \tag{2.9}$$

$$\Phi_l(C^{(0)}, \Gamma^{(0)}) = \delta_l \frac{\partial C^{(0)}}{\partial x} \quad \text{at} \quad x = 0, \tag{2.10a}$$

$$\Phi_g(C_s^{(0)}, \Gamma^{(0)}) = \delta_g(C_\infty - C_s^{(0)}) \quad \text{at} \quad x = 0, \tag{2.10b}$$

$$C^{(0)}(x,0) = C_0, \quad C_s^{(0)}(0) = C_\infty, \quad \Gamma^{(0)}(0) = 0, \tag{2.11a–c}$$

and the matching condition

$$C^{(0)}(x,t) = C_0 \quad \text{for} \quad x \to \infty. \tag{2.12}$$

In (2.10) $\delta_l = (D/T_c)^{1/2}/K_l$ and $\delta_g = E/K_g$. As such these parameters effectively represent the ratio of the time scales respectively characterizing the kinetic and diffusive stages of the adsorption process. (Thus $\delta \to 0, \infty$ respectively correspond to the 'diffusion-control' and 'kinetic-control' limits of this process.)

Following the standard approach (cf. Borwankar & Wasan 1983) we formally replace (2.10*a*) by the boundary condition

$$C^{(0)}(x,t) = C^{(0)}(0,t) \quad \text{at} \quad x = 0. \tag{2.13}$$

This enables separation of the above initial- and boundary-value problem into a linear problem governing $C^{(0)}(x,t)$ and a nonlinear problem for the evolution of $C^{(0)}(0,t)$ and $\Gamma^{(0)}(t)$. The former, consisting of (2.8), (2.11*a*), (2.12) and (2.13), allows the expression of $C^{(0)}(x,t)$ in terms of (the as yet unknown) $C^{(0)}(0,t)$ yielding

$$C^{(0)}(x,t) = C_0 + \int_0^t \frac{\partial C^{(0)}(0,\tau)}{\partial \tau}\,\mathrm{erfc}\left[\frac{x}{2(t-\tau)^{1/2}}\right]\mathrm{d}\tau, \tag{2.14a}$$

$$\left(\frac{\partial C^{(0)}}{\partial x}\right)_{x=0} = -\frac{1}{\pi^{1/2}}\int_0^t \frac{\partial C^{(0)}(0,\tau)}{\partial \tau}(t-\tau)^{-1/2}\,\mathrm{d}\tau. \tag{2.14b}$$

† In accordance with the above, C_0 and C_∞ both hereafter denote dimensionless concentrations appropriately normalized by $\overline{C}$. Thus, for instance, in the problem of an initially clean jet to be considered later on (cf. figure 1 and § 4.1) $C_0 = 0$ and $C_\infty = 1$.

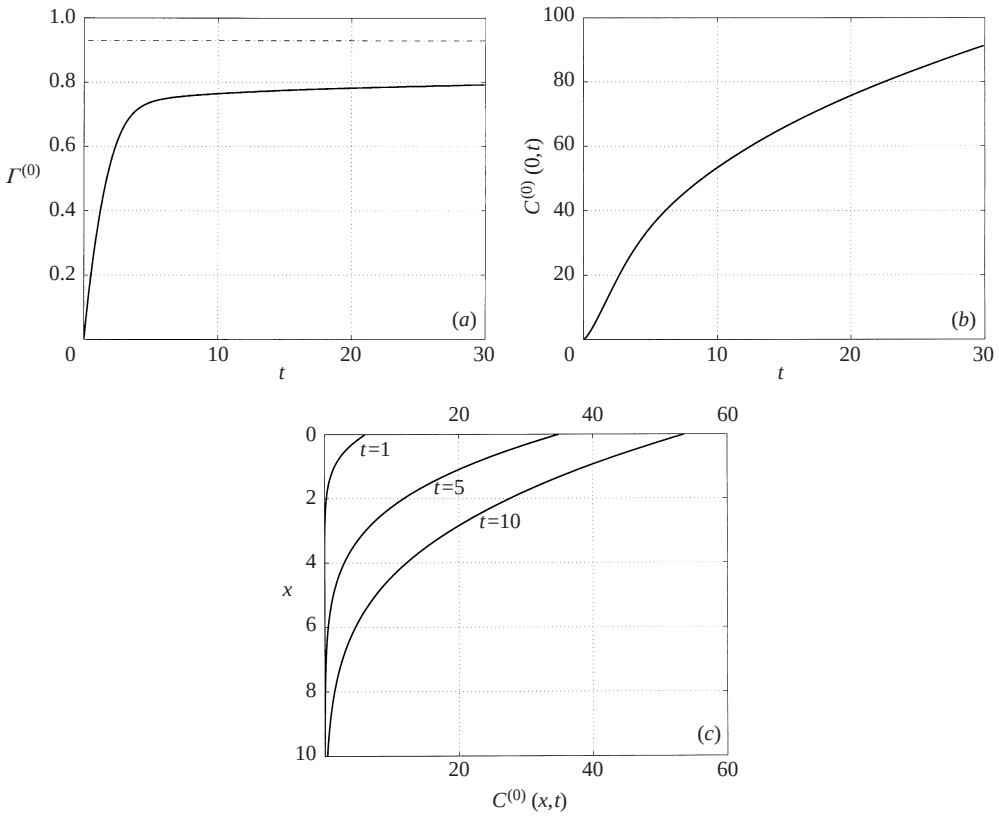

FIGURE 1. Evolution of the reference state for an initially clean jet for $\delta_l = 3.25$, $\delta_g = 0.085$, $\beta_l\overline{C} = 1.2 \times 10^{-2}$, $\beta_g\overline{C} = 13.2$, $(DT_c)^{1/2}\overline{C}/\Gamma_m = 1.6 \times 10^{-2}$ and $ET_c\overline{C}/\Gamma_m = 0.45$. (*a*) $\Gamma^{(0)}(t)$, the surface-excess concentration, (*b*) $C^{(0)}(0,t)$, the subsurface concentration and (*c*) $C^{(0)}(x,t)$, the bulk concentration distribution at the indicated instants of time.

Substituting the last expression in the respective right-hand sides of (2.9) and (2.10*a*) we obtain

$$\Phi_l(C^{(0)}, \Gamma^{(0)}) = -\frac{\delta_l}{\pi^{1/2}} \int_0^t \frac{\partial C^{(0)}(0,\tau)}{\partial \tau}(t-\tau)^{-1/2}\,\mathrm{d}\tau \tag{2.15}$$

and

$$\frac{\mathrm{d}\Gamma^{(0)}}{\mathrm{d}t} = -\frac{(DT_c)^{1/2}\overline{C}}{\pi^{1/2}\Gamma_m} \int_0^t \frac{\partial C^{(0)}(0,\tau)}{\partial \tau}(t-\tau)^{-1/2}\,\mathrm{d}\tau + \frac{ET_c\overline{C}}{\Gamma_m}(C_\infty - C_s^{(0)}), \tag{2.16}$$

which, together with (2.10*b*) and the initial conditions (2.11), serve to determine $\Gamma^{(0)}(t)$, $C_s^{(0)}(t)$ and $C^{(0)}(0,t)$ and thereby (via (2.14*a*)) $C^{(0)}(x,t)$ as well.

Figure 1 illustrates the evolution of the reference state whose stability is discussed in § 4. Thus parts (*a*) and (*b*) of this figure depict the time variation of $\Gamma^{(0)}(t)$ and $C^{(0)}(0,t)$, respectively, and part (*c*) presents $C^{(0)}(x,t)$ at the indicated instants. These correspond to an initially clean jet ($C_\infty = 1$ and $C_0 = 0$ in (2.11)) when adsorption is governed by the Langmuir-type relations (4.1) characterized by the dimensionless kinetic parameters $\delta_l = 3.25$, $\delta_g = 0.085$, $\beta_l\overline{C} = 1.2 \times 10^{-2}$ and $\beta_g\overline{C} = 13.2$. The mass transfer rates within each bulk phase respectively correspond to $(DT_c)^{1/2}\overline{C}/\Gamma_m = 1.6 \times 10^{-2}$ and $ET_c\overline{C}/\Gamma_m = 0.45$.

In figure 1(*a*) we observe that initially $\Gamma^{(0)}$ rises rapidly. At $t \approx 4$ it nearly reaches 75% of its steady-state equilibrium value marked by the horizontal dash–dotted asymptote. (At the same time, $t \approx 4$, the subsurface concentration, $C^{(0)}(0,t)$, presented in part (*b*), is less than 3% of its equilibrium value.) Subsequently, $\Gamma^{(0)}$ continues to rise slowly at a decreasing rate. It seems that at the early stages of the process the larger part of the solute flux from the surrounding atmosphere adsorbs to the freshly formed jet surface. Following this, when $\Gamma^{(0)}$ has increased sufficiently, the adsorption rate from the gas phase and desorption rate to the liquid side are nearly balanced. The latter desorption results in gradual increase of the subsurface concentration $C^{(0)}(0,t)$ and consequently, via bulk diffusion, of $C^{(0)}(x,t)$ as well (figure 1*c*). Owing to kinetic barriers and weak diffusion, relaxation of both is slow and, at $t = 10$, is still far from completion. Thus, contrary to the postulate put forward by Burkholder & Berg (1974), the boundary-layer-type reference-state distribution $C^{(0)}(x,t)$ is evidently both nonlinear and unsteady. Finally, we note that, once $\Gamma^{(0)}(t)$ becomes slowly varying and throughout the rest of the time interval presented, $C^{(0)}(0,t)$ is nearly proportional to $t^{1/2}$ and the substrate gradient $(\partial C^{(0)}/\partial x)_{x=0}$ varies only moderately. Both of these observations are related to the slow variation of $\Gamma^{(0)}(t)$ through solute mass balance at the jet surface. When $\Gamma^{(0)}(t)$ is slowly varying then, by (2.10*b*), so is $C_s^{(0)}(t)$. Consequently, from (2.9), solute fluxes within both bulk phases are slowly varying as well. Thus, since the diffusive boundary layer grows approximately as $\sim t^{1/2}$, the moderately changing $(\partial C^{(0)}/\partial x)_{x=0}$ is consistent with the observed variation of $C^{(0)}(0,t)$.

3. Evolution of perturbations

We assume that the surface of the jet

$$r = 1 + \eta(t)\cos kz \tag{3.1}$$

is perturbed by a small ($\eta \ll 1$) axisymmetric harmonic perturbation whose dimensionless wavenumber is k. Accordingly, all field variables are generically represented by

$$H(r,z,t) = H^{(0)}(r,t) + h(r,t)\begin{Bmatrix}\cos kz\\ \sin kz\end{Bmatrix},$$

in which $H^{(0)}$ corresponds to the reference state and the dimensionless perturbation amplitudes are presumed small ($h \ll H^{(0)}$). We wish to obtain the evolution equation governing $\eta(t)$. To this end we start by formulating and analysing the dynamic perturbation problem.

3.1. *The dynamic perturbation problem*

The radial and axial components (u,w) of the velocity perturbation amplitude and p, the pressure perturbation amplitude, satisfy the continuity equation

$$\frac{\partial u}{\partial r} + \frac{u}{r} + kw = 0 \tag{3.2}$$

and the linearized Navier–Stokes equations (for an otherwise quiescent jet)

$$\frac{\partial u}{\partial t} = -\frac{\partial p}{\partial r} + S\left(\frac{\partial^2 u}{\partial r^2} + \frac{1}{r}\frac{\partial u}{\partial r} - \frac{u}{r^2} - k^2 u\right) \tag{3.3}$$

and

$$\frac{\partial w}{\partial t} = kp + S\left(\frac{\partial^2 w}{\partial r^2} + \frac{1}{r}\frac{\partial w}{\partial r} - k^2 w\right), \tag{3.4}$$

in which

$$S = \frac{\mu}{(\rho a \sigma_0)^{1/2}},$$

where μ is the jet-liquid viscosity. As such S represents the ratio of the capillary (T_c) and viscous ($\rho a^2/\mu$) time scales. The above equations are supplemented by the (linearized) boundary conditions

$$u = \frac{\mathrm{d}\eta}{\mathrm{d}t} \quad \text{at} \quad r = 1, \tag{3.5}$$

$$u, \frac{\partial w}{\partial r} = 0 \quad \text{at} \quad r = 0, \tag{3.6}$$

$$p - S\frac{\partial u}{\partial r} = -\sigma(\Gamma^{(0)})(1 - k^2)\eta + \left(\frac{\partial \sigma}{\partial \Gamma}\right)^{(0)}\gamma \quad \text{at} \quad r = 1, \tag{3.7}$$

$$S\left(ku - \frac{\partial w}{\partial r}\right) = k\left(\frac{\partial \sigma}{\partial \Gamma}\right)^{(0)}\gamma \quad \text{at} \quad r = 1. \tag{3.8}$$

In (3.7) and (3.8) we have omitted the terms involving μ^s and κ^s, the shear and dilatational surface viscosities (while retaining bulk-viscosity terms). This is tantamount to assuming that the Boussinesq number $(\mu^s + \kappa^s)/\mu a \ll 1$, which is justified (cf. Scriven & Sternling 1964) for a relatively clean surface of a 1 mm water jet. Following the standard practice (Borwankar & Wasan 1983; MacLeod & Radke 1994) we postulate a general equilibrium surface equation of state which, for the presumed isothermal surface, specifies the surface-tension coefficient as a function $\sigma(\Gamma)$ of the instantaneous local surface-excess concentration. The perturbation amplitude of the surface-excess concentration γ therefore appears on the respective right-hand sides of the conditions (3.7) and (3.8) imposed upon the normal and shear stresses on the jet surface. Owing to this Marangoni effect, the above dynamic problem for the pressure and velocity perturbations is coupled to the transport problem considered in the next subsection.

The amplitude $\psi(r, t)$ of the Stokes stream function of the velocity perturbation satisfies

$$\frac{\partial^2 \psi}{\partial r^2} - \frac{1}{r}\frac{\partial \psi}{\partial r} - k^2 \psi = \zeta, \tag{3.9}$$

where $\zeta(r, t)/r$ is the amplitude of the vorticity perturbation which, from (3.3) and (3.4), is governed by

$$\frac{\partial \zeta}{\partial t} = S\left(\frac{\partial^2 \zeta}{\partial r^2} - \frac{1}{r}\frac{\partial \zeta}{\partial r} - k^2 \zeta\right), \tag{3.10}$$

together with the boundary conditions

$$\zeta(r, t), \frac{\partial \zeta}{\partial r}(r, t) = 0 \quad \text{at} \quad r = 0, \tag{3.11a, b}$$

$$\zeta(r, t) = k\left[\frac{1}{S}\left(\frac{\partial \sigma}{\partial \Gamma}\right)^{(0)}\gamma - 2\frac{\mathrm{d}\eta}{\mathrm{d}t}\right] \quad \text{at} \quad r = 1 \tag{3.12}$$

by (3.5), (3.8) and the definition of $\zeta(r,t)$. The solution of (3.9) satisfying (3.5) and (3.6) is

$$\psi(r,t)=\frac{rI_1(kr)}{kI_1}\frac{\mathrm{d}\eta}{\mathrm{d}t}+rI_1(kr)\left\{-\int_r^1 K_1(kr_1)\,\zeta(r_1,t)\,\mathrm{d}r_1\right.$$
$$\left.+\frac{K_1}{I_1}\int_0^1 I_1(kr_1)\,\zeta(r_1,t)\,\mathrm{d}r_1-\frac{K_1(kr)}{I_1(kr)}\int_0^r I_1(kr_1)\,\zeta(r_1,t)\,\mathrm{d}r_1\right\}, \quad (3.13)$$

wherein I_1 and K_1 respectively denote the modified Bessel functions of the first order and first and second kind. Whenever the arguments are explicitly omitted I_1 and K_1 are functions of k. From (3.13) and (3.4) we obtain (after a rather tedious calculation) $p(r,t)$ which, when substituted in the normal-stress condition (3.7) leads to

$$\frac{\mathrm{d}^2\eta}{\mathrm{d}t^2}+2S\left(2k^2-\frac{kI_1}{I_0}\right)\frac{\mathrm{d}\eta}{\mathrm{d}t}+\left(\frac{kI_1}{I_0}-k^2\right)\left(\frac{\partial\sigma}{\partial\Gamma}\right)^{(0)}\gamma$$
$$-\frac{kI_1}{I_0}(1-k^2)\,\sigma(\Gamma^{(0)})\,\eta=-\frac{2Sk^2}{I_0}\int_0^1 I_1(kr)\,\zeta(r,t)\,\mathrm{d}r. \quad (3.14)$$

In Appendix A we obtain $\zeta(r,t)$, the 'modified' vorticity perturbation, which, in turn, yields

$$\int_0^1 I_1(kr)\,\zeta(r,t)\,\mathrm{d}r=2kI_1\sum_{n=1}^{\infty}\frac{\alpha_n^2}{k^2+\alpha_n^2}$$
$$\times\int_0^t\left[\left(\frac{\partial\sigma}{\partial\Gamma}\right)^{(0)}\gamma(\tau)-2S\frac{\mathrm{d}\eta}{\mathrm{d}\tau}\right]\exp[-S(k^2+\alpha_n^2)(t-\tau)]\,\mathrm{d}\tau, \quad (3.15)$$

wherein α_n ($n=1,2,\ldots$) are the positive zeros of J_1. While (3.15) converges for all $S>0$, its convergence becomes dauntingly slow for $S\ll 1$, $k\sim O(1)$. In this limit we obtain from the asymptotic calculation in Appendix A

$$\int_0^1 I_1(kr)\,\zeta(r,t)\,\mathrm{d}r\sim 2kI_1S^{1/2}\int_0^t\left[\frac{1}{S}\left(\frac{\partial\sigma}{\partial\Gamma}\right)^{(0)}\gamma(\tau)-2\frac{\mathrm{d}\eta}{\mathrm{d}\tau}\right]$$
$$\times\left[\pi^{-1/2}(t-\tau)^{-1/2}-S^{1/2}\left(\frac{kI_1}{I_0}-\frac{1}{2}\right)+O(S)\right]\mathrm{d}\tau. \quad (3.16)$$

As has been anticipated (cf. (3.7), (3.8) *et seq.*), the equation obtained for $\eta(t)$, (3.14), depends both explicitly and implicitly (through the vorticity distribution, cf. (3.15) and (3.16)) on $\gamma(t)$, the surface concentration perturbation. To close the system of evolution equations we next address the perturbed solute transport.

3.2. *The transport perturbation problem*

Applying the same scaling as in the reference state we obtain (cf. Edwards, Brenner & Wasan 1991) the linearized perturbation equations

$$\frac{\partial c}{\partial t}+u\frac{\partial C^{(0)}}{\partial r}=\epsilon\left(\frac{\partial^2 c}{\partial r^2}+\frac{1}{r}\frac{\partial c}{\partial r}-k^2c\right)\quad\text{for}\quad 0<r<1, \quad (3.17)$$

$$\frac{\partial c}{\partial r}=0\quad\text{at}\quad r=0, \quad (3.18)$$

$$\frac{\mathrm{d}\gamma}{\mathrm{d}t} + \left(\frac{u}{r} + kw\right)\Gamma^{(0)} = -\frac{DT_c\overline{C}}{a\Gamma_m}\frac{\partial c}{\partial r} - \frac{ET_c\overline{C}}{\Gamma_m}c_s \quad \text{at} \quad r = 1, \tag{3.19}$$

$$\left(\frac{\partial \Phi_l}{\partial C}\right)^{(0)} c + \left(\frac{\partial \Phi_l}{\partial \Gamma}\right)^{(0)} \gamma = -\delta_l \epsilon^{1/2}\frac{\partial c}{\partial r} \quad \text{at} \quad r = 1, \tag{3.20a}$$

$$\left(\frac{\partial \Phi_g}{\partial C}\right)^{(0)} c_s + \left(\frac{\partial \Phi_g}{\partial \Gamma}\right)^{(0)} \gamma = -\delta_g c_s \quad \text{at} \quad r = 1, \tag{3.20b}$$

together with appropriate initial conditions. In the above c and c_s respectively denote the perturbation amplitudes of the bulk concentration distribution within the jet and the concentration at its outer surface. Surface diffusion would manifest itself through the appearance on the right-hand side of (3.19) of the term $-k^2(D^s/D)\epsilon\gamma$ omitted above, where D^s denotes the coefficient of surface diffusivity. Inspection of the following asymptotic calculation reveals that the omitted term is too small to affect the resulting evolution equations.

Since γ appearing in (3.14) depends (through the surface mass balance and adsorption relations) upon the bulk concentration and velocity perturbations in the vicinity of the jet surface, we focus on the 'inner' limit of the transport problem. In terms of the 'inner' variable x (cf. (2.7)), the transport equation governing c is (to leading order in $\epsilon \ll 1$)

$$\frac{\partial c}{\partial t} - \epsilon^{-1/2}u(x,t)\frac{\partial C^{(0)}}{\partial x} = \frac{\partial^2 c}{\partial x^2}. \tag{3.21}$$

The large $O(\epsilon^{-1/2})$ convection term appearing on the left-hand side originates from the fact that $C^{(0)}$, the reference concentration distribution, varies on the $O(\epsilon^{1/2})$ scale of the boundary layer. Thus, even the small $O(\eta)$ radial perturbation velocity imposed by the jet-surface displacement (3.5) is capable of creating a large radial solute flux. The dominant balance (3.21) therefore suggests the expansion

$$c(x,t;\epsilon) \sim \epsilon^{-1/2}c_0(x,t)[1 + O(\epsilon^{1/2})]$$

(wherein c_0 is presumed $O(\eta)$). The leading-order $c_0(x,t)$ is governed by

$$\frac{\partial c_0}{\partial t} - \frac{\partial^2 c_0}{\partial x^2} = u(x,t)\frac{\partial C^{(0)}}{\partial x}. \tag{3.22a}$$

This is supplemented by the boundary condition

$$\left(\frac{\partial \Phi_l}{\partial C}\right)^{(0)} c_0 - \delta_l\frac{\partial c_0}{\partial x} + \epsilon^{1/2}\left(\frac{\partial \Phi_l}{\partial \Gamma}\right)^{(0)} \gamma = 0 \quad \text{at} \quad x = 0, \tag{3.22b}$$

and the homogeneous† initial and matching conditions

$$c_0(x,0) = 0, \tag{3.22c}$$

$$c_0(x,t) = 0 \quad \text{as} \quad x \to \infty. \tag{3.22d}$$

Solution of the above problem is obtained by presenting $c_0(x,t)$ as the sum

$$c_0 = c_{01} + c_{02}, \tag{3.23}$$

† There is no *a priori* reason to anticipate initial concentration perturbations larger than the presumed $O(\eta)$ velocity and pressure perturbations, see also (A 1) *et seq.* Additionally, the last term is retained in (3.22*b*) despite the appearance of the $\epsilon^{1/2}$ factor. In certain cases the numerical value of $(\partial\Phi_l/\partial\Gamma)^{(0)}$ may be sufficiently large to make the contribution of this term non-negligible.

wherein c_{01} satisfies (3.22a, c, d) and $c_{01}(0,t) = 0$ whereas c_{02} satisfies the homogeneous equation associated with (3.22a) together with (3.22c, d) and the condition resulting from substitution of (3.23) into (3.22b).

For the first term in (3.23) we thus obtain

$$c_{01}(x,t) = \int_0^t \int_0^\infty G(x,t,x_0,t_0) u(x_0,t_0) \frac{\partial C^{(0)}}{\partial x_0}(x_0,t_0)\,\mathrm{d}x_0\,\mathrm{d}t_0 \tag{3.24a}$$

in which the appropriate Green's function is

$$G(x,t,x_0,t_0) = \tfrac{1}{2}[\pi(t-t_0)]^{-1/2}\left\{\exp\left[-\frac{(x-x_0)^2}{4(t-t_0)}\right] - \exp\left[-\frac{(x+x_0)^2}{4(t-t_0)}\right]\right\} \tag{3.24b}$$

(for $t > t_0$). Subsequent derivation may proceed via substitution of

$$u = \frac{k}{r}\psi = \frac{I_1(kr)}{I_1}\frac{\mathrm{d}\eta}{\mathrm{d}t} + kI_1(kr)\left\{-\int_r^1 K_1(kr_1)\zeta(r_1,t)\,\mathrm{d}r_1 + \frac{K_1}{I_1}\int_0^1 I_1(kr_1)\zeta(r_1,t)\,\mathrm{d}r_1 - \frac{K_1(kr)}{I_1(kr)}\int_0^r I_1(kr_1)\zeta(r_1,t)\,\mathrm{d}r_1\right\} \tag{3.25}$$

(cf. (3.13)) together with $\zeta(r,t)$ (A 2). Considerable simplification of the resulting evolution equation is however gained by recalling that, unlike the transport problem, the dynamic problem is explicitly independent of ϵ. As such the latter problem does not yield an $O(\epsilon^{1/2})$ boundary-layer solution. (Note, however, that an $O(S^{1/2})$ *dynamic* boundary layer does form near the jet surface in the limit $S \ll 1$, as may be verified from (3.25) in conjunction with (A 5). However, since in all physically relevant situations $S \gg \epsilon$ (cf. Appendix B), variations of u still take place on a scale much larger than that of the above transport boundary layer. The approximation (3.26) thus remains valid at $S \ll 1$ with the error estimate appropriately modified to $O(\epsilon^{1/2}/S^{1/2})$.) Transforming (3.25) to the inner variable x, we readily verify that

$$u(x,t) \sim \frac{\mathrm{d}\eta}{\mathrm{d}t}[1 + O(\epsilon^{1/2})], \tag{3.26}$$

in agreement with (3.5). Hence, to leading order

$$c_{01}(x,t) = \int_0^t \int_0^\infty G(x,t,x_0,t_0)\frac{\mathrm{d}\eta}{\mathrm{d}t_0}\frac{\partial C^{(0)}}{\partial x_0}(x_0,t_0)\,\mathrm{d}x_0\,\mathrm{d}t_0. \tag{3.27}$$

Similarly to the calculation of the reference state $C^{(0)}(x,t)$, we express $(\partial c_{02}/\partial x)_{x=0}$ in terms of the yet unknown function $c_{02}(0,t)$ (cf. (2.14)). Substituting this and c_{01} into (3.22b) we eventually obtain the evolution equation

$$\left(\frac{\partial \Phi_l}{\partial C}\right)^{(0)} c_{02}(0,t) + \epsilon^{1/2}\left(\frac{\partial \Phi_l}{\partial \Gamma}\right)^{(0)}\gamma(t) + \frac{\delta_l}{\pi^{1/2}}\int_0^t \frac{\partial c_{02}}{\partial \tau}(0,\tau)(t-\tau)^{-1/2}\,\mathrm{d}\tau = -\frac{\delta_l}{\pi}\int_0^t \mathrm{d}t_1 \frac{\mathrm{d}\eta}{\mathrm{d}t_1}(t-t_1)^{-1/2}\int_0^{t_1}\mathrm{d}t_2 \frac{\partial C^{(0)}}{\partial t_2}(0,t_2)\frac{(t_1-t_2)^{1/2}}{t-t_2}. \tag{3.28}$$

To obtain a closed set of evolution equations for $\eta(t)$, $\gamma(t)$ and $c_{02}(0,t)$ we need to consider the surface mass balance (3.19) in conjunction with the dynamic perturbation problem. Writing (3.19) in terms of the inner variable x, we obtain

$$\frac{\mathrm{d}\gamma}{\mathrm{d}t} + \frac{E T_c \overline{C}}{\Gamma_m} c_s = -\left(\frac{u}{r} + kw\right)\Gamma^{(0)} + \frac{\overline{C}a}{\Gamma_m}\frac{\partial c_0}{\partial x} \quad \text{at} \quad x = 0. \tag{3.29}$$

Making use of (3.20*b*) to express c_s in terms of γ, (3.13) to obtain $u/r + kw$ at $r = 1$ and substituting these together with the expression for $\partial c_0/\partial x$ at $x = 0$ obtained in the course of deriving (3.28) (cf. (3.24) *et seq.*), we eventually arrive at

$$\frac{\mathrm{d}\gamma}{\mathrm{d}t} - \frac{E T_c \overline{C}}{\Gamma_m} \frac{(\partial \Phi_g/\partial \Gamma)^{(0)}}{\delta_g + (\partial \Phi_g/\partial C)^{(0)}} \gamma$$

$$= \left[\left(\frac{kI_0}{I_1} - 1 \right) \frac{\mathrm{d}\eta}{\mathrm{d}t} + \frac{k}{I_1} \int_0^1 I_1(kr) \zeta(r,t)\, \mathrm{d}r \right] \Gamma^{(0)}$$

$$- \frac{\overline{C} a}{\Gamma_m} \left\{ \frac{1}{\pi^{1/2}} \int_0^t \frac{\partial c_{02}}{\partial \tau}(0,\tau)\, (t-\tau)^{-1/2}\, \mathrm{d}\tau \right.$$

$$\left. + \frac{1}{\pi} \int_0^t \mathrm{d}t_1 \frac{\mathrm{d}\eta}{\mathrm{d}t_1}(t-t_1)^{-1/2} \int_0^{t_1} \mathrm{d}\tau \frac{\partial C^{(0)}}{\partial \tau}(0,\tau) \frac{(t_1-\tau)^{1/2}}{t-\tau} \right\}. \tag{3.30}$$

Equations (3.14), (3.28) and (3.30) supplemented by (3.15) or (3.16) constitute a system of coupled Volterra-type integro-differential equations governing the evolution of $\eta(t)$, $c_{02}(0,t)$ and $\gamma(t)$.

4. Results and discussion

The above equations involve the instantaneous values of η, γ, c_{02} and their time derivatives as well as (explicitly and implicitly) their past evolution. The implicit 'memory effect' is associated with the integrations of the vorticity distribution appearing on the respective right-hand sides of (3.14) and (3.30). This effect originates from the dependence of the vorticity source on the perturbed jet surface upon the instantaneous values of $\mathrm{d}\eta/\mathrm{d}t$ and γ, (3.12), together with the fact that (for all finite values of S) the evolution of the bulk vorticity distribution through inwards diffusion from the surface is not instantaneous (cf. Prosperetti 1977; Frankel & Weihs 1987). The explicit convolution integrals appearing in both (3.28) and (3.30) reflect the effect on solute diffusive flux perturbation of the evolution of the solute concentration gradient in the unsteady reference state.

Our first objective is to identify the mechanism by which solute mass transfer triggers the Marangoni instability in the present problem. While equations (3.14), (3.15), (3.28) and (3.30) have been derived for arbitrary S, the values of S occurring in actual applications are often relatively small (cf. Appendix B). The subsequent discussion therefore focuses on these cases.

Consider to begin with (monotonical) divergence of perturbations. From (3.16) we conclude that when $S \ll 1$ the evolution of $\eta(t)$ is governed by the balance of the third and fourth terms on the left-hand side of (3.14). (Numerical evidence indicates that this is essentially correct throughout the entire domain of S values considered here.) The latter term represents the standard Rayleigh effect (though with a variable surface-tension coefficient owing to unsteadiness of the reference state) resulting from perturbation of the jet surface curvature. As such, this term has a stabilizing (restoring) or destabilizing effect according to whether $k > 1$ or $k < 1$, respectively. The term linear in γ represents the Marangoni effect associated with non-uniformity of the surface tension. This term combines contributions from both the last term on the right-hand side of (3.7) and the pressure perturbation (proportional to kI_1/I_0 and k^2, respectively). Since $kI_0/I_1 > 1$ for all $k > 0$, the latter contribution dominates. Thus, for surface-tension-reducing solutes (i.e. when $(\partial\sigma/\partial\Gamma)^{(0)} < 0$), a surface-excess

concentration perturbation γ whose sign is opposite to that of the surface displacement (i.e. one increasing solute concentration at the troughs and decreasing it at the crests) will give rise to a destabilizing Marangoni effect for all wavelengths.

The feasibility of such a persisting $\gamma(t)$ is now examined by considering the various contributions appearing in (3.29) or (3.30) (both representing solute mass balance at the perturbed jet surface). Since for an arbitrary adsorption relation $(\partial\Phi/\partial\Gamma)^{(0)} < 0$ and $(\partial\Phi/\partial C)^{(0)} > 0$ (cf. Borwankar & Wasan 1983), the mass-transfer term on the left-hand side of (3.30) is stabilizing. Evidently, a larger (dimensionless) mass-transfer rate $ET_c\overline{C}/\Gamma_m$ will tend to eliminate increasingly rapidly any concentration perturbation occurring in the vicinity of the jet surface. However, as we shall presently see, solute mass transfer may have a substantial (though indirect) destabilizing effect.

The first expression on the right-hand side of (3.30) represents the effect of surface convection (cf. Edwards *et al.* 1991). This expression depends explicitly upon $\mathrm{d}\eta/\mathrm{d}t$ and implicitly, through the vorticity distribution (cf. (3.15)), upon both $\mathrm{d}\eta/\mathrm{d}t$ and γ. The contribution of the former is dominated by the explicit term which, in turn, describes the rate of jet-surface contraction as a result of the irrotational flow corresponding to the prescribed jet-surface perturbation. Thus, for instance, for $\mathrm{d}\eta/\mathrm{d}t > 0$ (and $\eta > 0$), the surface contracts at the crests and dilates at the troughs thereby tending to induce $\gamma > 0$ contributing, as explained above, to a stabilizing Marangoni effect in (3.14). Finally, the (implicit) dependence upon γ corresponds to surface convection directly induced by non-uniform surface tension resulting from non-uniform surface-excess concentration. For surface-tension-reducing agents this surface convection acts to eliminate γ and restore uniformity of adsorbed solute concentration. For future reference we note that in the limit $S \to 0$ (cf. (3.16)) this effect may become $O(S^{-1/2})$ large.

The sum of the two terms in the braces appearing on the right-hand side of (3.30) explicitly represents the opposing contributions of c_{01} and c_{02} (cf. (3.23)) to the diffusion term (the last on the right-hand side) of (3.29). This term together with the Marangoni term in (3.14) form the main link coupling the evolution of the jet-surface displacement and solute-concentration perturbation. As may readily be seen from (3.24), for $\mathrm{d}\eta/\mathrm{d}t > 0$ (and $\eta > 0$), the sign of the second term in the braces (which dominates the contribution of c_{02}) is determined by $\partial C^{(0)}/\partial x$. In the case of an initially clean jet in a contaminated atmosphere, solute mass transfer will take place into the jet yielding $\partial C^{(0)}/\partial x < 0$ (cf. figure 1). The diffusion term will then act to produce a surface-excess perturbation $\gamma < 0$ thereby giving rise to a destabilizing Marangoni effect in (3.14). When the direction of solute mass flux in the reference state is outwards (e.g. a contaminated jet discharging into an initially clean atmosphere), the effect of diffusion will be stabilizing. The correction c_{02} originates from the boundary condition (3.22*b*) which, in general, is not satisfied by c_{01} alone. This correction gives rise to the penultimate term on the right-hand side of (3.30) acting to diminish the magnitude of the perturbation diffusive flux.

Further physical insight into the present problem may be gained by considering the source of the diffusion term in (3.29). The forcing term on the right-hand side of (3.22*a*) indicates that the perturbation diffusive flux is generated via convection by the radial velocity perturbation (induced, in turn, by displacement of the perturbed jet surface) across the reference-state boundary-layer distribution. When $\partial C^{(0)}/\partial x < 0$ and $\mathrm{d}\eta/\mathrm{d}t > 0$ the radial convection acts to reduce the local bulk solute concentration in the vicinity of the crests of the perturbed jet surface. Indeed, $c_{01} < 0$ for all $x > 0$ (cf. (3.24)). This (in conjunction with the vanishing of $c_{01}(0,t)$) yields the substrate gradient $\partial c_{01}/\partial x < 0$ and the accompanying diffusive flux. The latter acts to reduce the

surface-excess concentration in the vicinity of the crests, i.e. generate the perturbation $\gamma < 0$.

As mentioned above, the correction c_{02} originates from the condition (3.22*b*) which imposes equality of the diffusive flux and adsorption rate on the liquid side of the jet surface. From this balance it follows that both reduced desorption rate and occurrence of inwards diffusive flux (respectively associated with $\gamma < 0$ and $\partial c_{01}/\partial x < 0$) result in reduced subsurface concentration , i.e. $c_{02}(0, t) < 0$. This, in turn, acts to diminish the inwards diffusive flux. The corresponding contribution of c_{02} in (3.30) is thus the present version of a 'back diffusion' term (cf. Eastoe & Dalton 2000).

The foregoing discussion supersedes in the context of the present well-posed initial-value perturbation problem the somewhat incoherent rationalization previously advanced by Burkholder & Berg (1974). Finally, it is worthwhile to note that the above is closely analogous to the mechanisms respectively proposed by Pearson (1958) and Sternling & Scriven (1959) for surface-tension-induced cellular convection. We further comment on this analogy in § 5.

4.1. *An illustration: a Langmuir–Hinshelwood system*

The effect of solute mass transfer on jet stability will now be illustrated for systems satisfying Langmuir–Hinshelwood-type kinetic expressions

$$\Phi_i(C, \Gamma) = C(1 - \Gamma) - \Gamma/\beta_i \overline{C}, \quad i = l, g \tag{4.1}$$

(which at equilibrium reduce to the Langmuir isotherm), together with the accompanying surface equation of state

$$\sigma(\Gamma) = 1 + M \log(1 - \Gamma). \tag{4.2}$$

These relatively simple nonlinear relations adequately describe the kinetics of aqueous solutions of the lower-molecular-weight alcohols (which are both volatile and significantly soluble). Appearing in the above are β_l and β_g representing the surface activity of the solute (see Appendix B) as well as the Marangoni parameter $M = R\Theta\Gamma_m/\sigma_0$ in which R denotes the universal gas constant and Θ is the absolute temperature.

Owing to the unsteadiness of the reference state, one needs to solve the initial-value problem for the evolution of perturbations rather than the standard eigenvalue problem for the growth rate. To this end (3.14), (3.28) and (3.30) have been integrated numerically subject to the initial conditions $\eta(0) = 1$, $\eta'(0) = 0$, $\gamma(0) = -1$ and $c_{02}(0, 0) = 0$. Typical of unsteady flows is that their instability is not dominated at all times by a single 'fastest-growing' perturbation. Rather, different wavenumbers assume the lead at different times (cf. Frankel & Weihs 1987). The initial-value problem for the evolution of perturbations has therefore been integrated for a large number of dimensionless wavenumbers k. This enables the description of the time variation of $\eta_m(t)$, the growth of the instantaneously most amplified surface perturbations, together with the values of the corresponding dimensionless wavenumbers $k_m(t)$. We focus on the case of an initially clean jet ($C_0 = 0$ in (2.1*a*)) in which, according to the above general discussion, solute mass transfer yields the most destabilizing Marangoni effect. The solute mass transfer within both phases and the kinetics of adsorption are characterized by the set of parameters previously mentioned in the context of figure 1 together with $\overline{C}a/\Gamma_m = 8.1$.

Figure 2 describes the effect of S on the amplification of perturbations. We present the variation with time of η_m and the corresponding k_m for $M = 0.6$ and the indicated values of S. The dashed line in part (*a*) represents the most amplified mode in the Rayleigh instability of a clean inviscid jet (characterized by the same capillary time

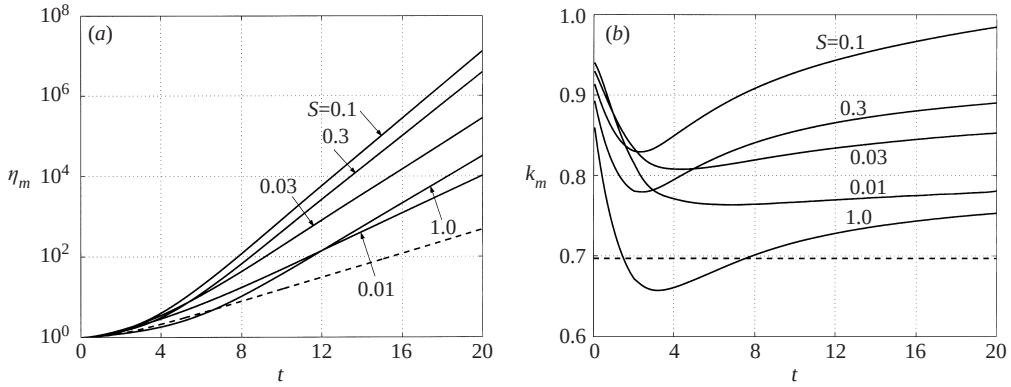

FIGURE 2. Effect of S on the evolution of (a) η_m and (b) k_m of the instantaneously most amplified perturbations for $M = 0.6$ and $\overline{C}a/\Gamma_m = 8.1$. All other parameters the same as in figure 1. Dashed lines depict the corresponding most unstable Rayleigh mode.

scale T_c). The latter shows a substantially smaller perturbation growth than in all other cases presented. This seems remarkable given that the Rayleigh case is free of viscous damping. Furthermore, according to (4.2) and figure 1(a), in all other cases the surface tension decreases with time (by more than 30% at $t \approx 4$ and eventually by nearly 70%). We therefore conclude that the main source of instability in the present problem is the Marangoni mechanism associated with solute mass transfer which more than compensates for the reduced Rayleigh instability.

Another interesting feature is that, unlike the comparable problem of a clean system (i.e. in the absence of Marangoni effect), η_m here varies non-monotonically with S. With decreasing S, η_m initially grows and then, below $S = 0.1$, the trend changes and η_m decreases with further decrease of S. (For smaller values of M this trend reversal appears at smaller values of S.) The former trend is associated with the expected diminution of the damping term (second on the left-hand side) of (3.14), which is the prevailing influence at relatively large values of S. Then, for small S ($\ll 1$, see (3.16)), the expression

$$\frac{k^2\Gamma^{(0)}(t)}{\pi^{1/2}S^{1/2}}\int_0^1\left(\frac{\partial\sigma}{\partial\Gamma}\right)^{(0)}\frac{\gamma(\tau)}{(t-\tau)^{1/2}}\,\mathrm{d}\tau \tag{4.3}$$

emerges as the leading behaviour of the surface-convection term on the right-hand side of (3.30). This causes the rapid attenuation of γ thereby eliminating the Marangoni term (third on the left-hand side) of (3.14). The origin of this mechanism may be traced back to (3.8). In the presence of surfactants the condition imposed upon the shear stresses at the surface of the jet becomes singular in the limit $S \to 0$. This singularity reflects the fact that, in the absence of viscosity, the bulk fluid cannot sustain the shear stresses created by the perturbations of surface-excess concentration. The non-uniformity of surface tension then immediately eliminates the perturbation of adsorbed solute concentration.

All curves presented in figure 2 (b) show that the corresponding values of k_m initially decrease and then increase slowly, approaching respectively constant long-time limits. These limits are considerably larger than Rayleigh's value (0.697, marked by the horizontal dashed line) corresponding to a clean inviscid jet. Furthermore, similarly to the behaviour of η_m observed above, the variation of k_m with S is non-monotonical. Thus, for $S < 0.1$, k_m decreases with S, i.e. contrary to a clean jet, reduced viscosity

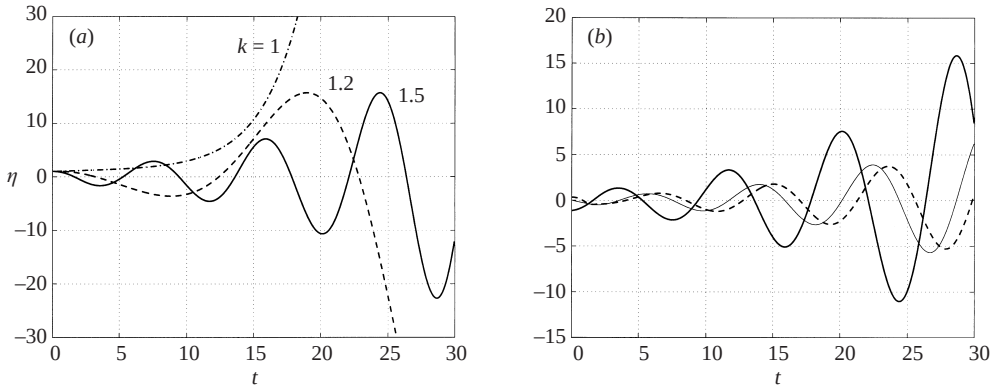

FIGURE 3. (*a*) Oscillatory amplifications of perturbations for the indicated $k(\geqslant 1)$ values. (*b*) Time dependence of —, Rayleigh term; - - -, Marangoni term; and —, $\eta'(t)$ for $k = 1.5$. In both parts $M = 0.24$, $S = 0.003$ and all other parameters the same as in figure 2.

results in increasing wavelength of the dominant perturbations. Both the magnitude and mode of variation of k_m with S are related to the Marangoni effect. Thus, we note that increasing k increases the magnitude of the coefficient of the Marangoni term in (3.14). The values of k_m are therefore larger than those for clean jets of comparable viscosity. For $S \ll 1$ the surface-convection term (4.3) which is proportional to k^2 becomes dominant. Consequently, the values of k_m eventually decrease with S.

The constant limits of k_m and the nearly linear variation of $\log \eta_m$ at long times correspond to approximately exponential long-time growth of perturbations which, in turn, indicates that the transient problem has evolved into a quasi-steady one. These trends are in agreement with the previously observed (cf. figure 1) slow long-time variation of $\Gamma^{(0)}$ and $(\partial C^{(0)}/\partial x)_{x=0}$ in the reference state as well as the fading (approximately as $t^{-1/2}$) of the early-time contributions to the memory terms in the above evolution equations.

Another interesting feature of the present problem is the occurrence of amplified oscillations. These are illustrated in figure 3(*a*) depicting $\eta(t)$ for $M = 0.24$, $S = 0.003$ and the indicated wavenumbers $k \geqslant 1$. (All other parameters remain the same as in figure 2.) At $k = 1$, $\eta(t)$ still grows monotonically as a result of a destabilizing Marangoni effect. (The Rayleigh term is now absent from (3.14).) For $k = 1.2$ and $k = 1.5$ perturbations grow through oscillations of increasing amplitude. In the absence of Marangoni effect, the oscillatory perturbations pertaining to $k > 1$ are damped by viscous dissipation for all (however small) $S > 0$. It therefore seems worthwhile to clarify the mechanism underlying the observed amplification. As argued at the very beginning of this section, at the relatively small values of S considered here, $\eta(t)$ is essentially dominated by the balance of the Marangoni and Rayleigh effects. The bold solid and dashed curves in figure 3(*b*) respectively present the time variation of the Rayleigh and Marangoni terms of (3.14) for $k = 1.5$ and M, S the same as in part (*a*) of the figure. The thin solid line is proportional to $\eta'(t)$. Typical of all $k > 1$ is that the amplitude of the restoring (linear in η) Rayleigh term exceeds that of the Marangoni term, the time dependence being therefore oscillatory. However, the latter term is nearly in phase with $\eta'(t)$ which gives rise to a resonance interaction: The Marangoni term in (3.14) enhances $|\mathrm{d}\eta/\mathrm{d}t|$ which, in turn, augments the destabilizing diffusion term in (3.30). An overstability mechanism (cf. Chandrasekhar 1961) is thereby generated. (For still larger values of $k > 1$, enhanced viscous damp-

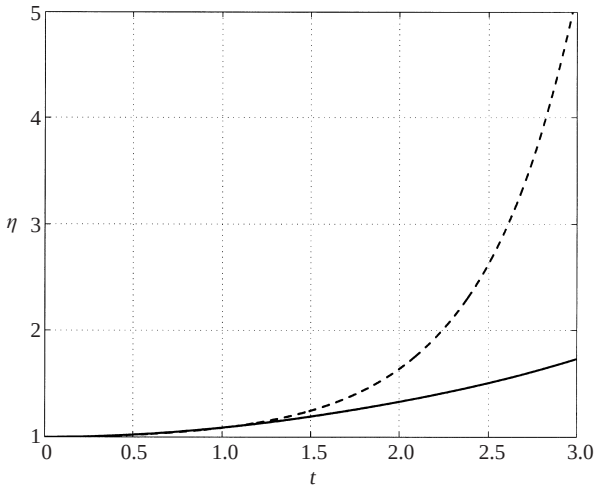

FIGURE 4. Evolution of $\eta(t)$: —, actual ($\delta_l = 3.25$); - - -, diffusion-control approximation ($\delta_l = 0$) for $k = 0.8$ and all other parameters the same as in figure 3.

ing will eventually prevail and diminish $|\mathrm{d}\eta/\mathrm{d}t|$. This, accompanied by the further enhancement of the attenuating surface-convection term (4.3) in (3.30), will cause the subsidence of both γ and η oscillations.)

Actual data regarding K_l, the kinetic rate constant, are generally lacking, which makes it difficult to estimate the parameter δ_l. This difficulty is commonly avoided by adopting the 'diffusion-control' limit $\delta_l \to 0$ (i.e. assuming infinitely fast kinetics). In this limit, the diffusive flux terms vanish from (2.10) and (3.20) which thereby reduce to the corresponding equilibrium relations, significantly simplifying the ensuing analysis. We now turn to consider the effect on jet stability of the parameter δ_l. The discussion will also serve to examine the adequacy in the present problem of the prevailing diffusion-control approximation.

In the case of an initially clean jet, a reduced diffusion rate or increased kinetic transfer rate are expected to result in increased subsurface concentration $C^{(0)}(0,t)$ (the slow diffusion being incapable of transferring the solute released by desorption into the bulk of the jet sufficiently rapidly). This, in turn, increases the gradient $\partial C^{(0)}/\partial x$ thereby enhancing the Marangoni instability. Consequently, the diffusion-control limit provides an upper bound to the Marangoni instability whereas this type of instability vanishes in the limit $\delta_l \to \infty$ of kinetic (or transfer) control.

Figure 4 compares the actual evolution of $\eta(t)$ (solid line, $\delta_l = 3.25$) for $k = 0.8$ and all other parameters the same as in figure 3 to the evolution predicted by the diffusion-control limit (dashed line, $\delta_l = 0$). The value $\delta_l = 3.25$ approximates the data (cf. Appendix B) for the system hexanol–water–air which is 'mixed-control' (Joos & Serrien 1989; Chang & Franses 1995). The corresponding $\eta(t)$ is indeed much smaller than that predicted by the diffusion-control limit. In a homologous solute series the adsorption rate constants increase with the length of the molecular chain while the diffusivities moderately decrease. The value of δ_l thus decreases, which apparently indicates an increasing Marangoni instability with increasing molecular weight of solute. While this is true of aqueous solutions of the lower-molecular-weight homologues, the rapidly diminishing solubility results in the vanishing of the parameter $\overline{C}a/\Gamma_m$ in (3.29) and (3.30). Thus, the diffusion term which constitutes an essential link in the Marangoni instability associated with solute mass transfer

is eventually eliminated altogether. Indeed, the present mixed-control system for which $\delta_l \approx 3.25$ (cf. Appendix B) is far more susceptible to Marangoni instability than systems such as decanol–water–air for which (cf. MacLeod & Radke 1994) $\delta_l \approx 1.2 \times 10^{-2}$ despite the fact that the latter are much closer to the diffusion-control limit.

5. Concluding remarks

The main thrust of the present contribution has been the relaxation of the *ad hoc* steadiness assumption impairing previous analyses. The inherent unsteadiness of the problem originates from the initial lack of equilibrium between the two bulk phases as well as between each of them and the freshly formed jet surface. Thus, for instance, despite the small solute diffusivity in the liquid phase, diffusion there is non-uniformly weak and slow. Rather, within the boundary layer developing near the jet surface, significant diffusive flux and concentration variations take place on the time scale of perturbation evolution. The same is true of the surface-excess concentration (see figure 1).

In this context Tarr & Berg (1980) reported substantial deviations of their results from those of Burkholder & Berg (1974) unless the concentration boundary-layer thickness exceeded about 1% of the jet radius. Comparison with figure 1(*c*) in conjunction with the definition (2.7) of the inner variable reveals that, for $\epsilon \approx 10^{-6}$, this is not achieved until $t \approx 10$. In view of the present analysis it is thus hardly surprising that Tarr & Berg (1980) suggested that according to experimental data (and contrary to the steadiness assumption) '. . . jet breakup during mass transfer may be controlled by the concentration profile existing during the very early stages of jet life, when the diffusion boundary layer is extremely thin.'

It has been observed (cf. the discussion at the conclusion of § 2) that, at sufficiently long times ($t \gtrsim 10$), the reference state becomes slowly varying insofar as the elements affecting the growth of perturbations are concerned. Indeed (see figure 2*a*), at these times perturbations grow nearly exponentially. However, during the preceding interval ($0 < t \lesssim 10$) perturbations have experienced a substantial but non-uniform growth (depending on the respective wavenumbers). Consequently, even at $t \gtrsim 10$, the wavenumbers k_m corresponding to the instantaneously most amplified perturbations still vary (figure 2*b*). There thus seems no way whereby the above initial-value stability analysis could consistently be replaced by the standard eigenvalue approach (see Berger 1988, and the footnote at the Introduction).

Another consequence of the initial lack of equilibrium between the solute concentrations at the various phases is the relative importance of solute mass transfer within the gaseous phase. This is usually estimated (Hansen 1960; MacLeod & Radke 1994) by the ratio $K_p(D_g/D)^{1/2}$ ($\approx 8.6 \times 10^{-2}$ for the system illustrated, cf. Appendix B). This assessment, which assumes an equilibrium ratio of the respective concentrations within the gaseous and liquid phases, is inapplicable to the problem of the initially clean jet on which we have focused. Rather, in this case, the ratio of the diffusive fluxes is approximately $[C_\infty - C_s^{(0)}(t)]/C^{(0)}(0,t) \times (D_g/D)^{1/2}$ which (figure 1(*b*)) is gradually decreasing from a large initial (at $t \to 0^+$) value, only becoming $O(1)$ at $t \approx 1$ and remaining at this order throughout the rest of the time interval considered.

In the present problem capillarity may give rise to instability through the Rayleigh mechanism or the Marangoni effect induced by non-uniformity of surface tension. The latter mechanism is analogous to that proposed by Pearson (1958) and Sernling & Scriven (1959) for the onset of cellular convection. In both cases the driving force

of instability is the lack of thermal or chemical equilibrium between the fluid and adjacent medium resulting in temperature or concentration gradients across the jet or fluid layer. Perturbative convection across these gradients perturbs the interfacial temperature or concentration thereby generating a non-uniform surface tension and accompanying surface tractions which may, depending on the gradient direction, act to further enhance bulk fluid motion. Solute adsorption somewhat complicates the chain of events in the present problem. Thus perturbation of surface-excess concentration (and hence changes of surface tension) are only indirectly effected by the radial velocity perturbation through the generation of a diffusive solute flux at the bulk substrate.

It has been demonstrated (cf. figure 4) that the commonly assumed diffusion-control approximation is inapplicable to the description of the system hexanol–water–air (which is known to be of mixed-control type, Joos & Serrien 1989). Additional results (not presented here) indicate that this approximation is inadequate even for systems characterized by δ_l with a value an order of magnitude smaller than that of the above (≈ 3.25). Indeed, the approach to the diffusion-control limit is expected to be rather slow. Unless the initial solute distribution corresponds to a state of equilibrium, the equilibrium limit $\delta_l \to 0$ will be non-uniform on an $O(\delta_l^2)$ time scale when diffusive fluxes resulting from large initial concentration gradients are significant. Furthermore, owing to the occurrence of 'memory effects' in the evolution equations, this initial non-uniformity may have a global long-term effect for all $\delta_l > 0$.

The authors are grateful to a referee who pointed out an error in the original formulation of the solute mass balance at the jet surface. This research was supported by the Israel Science Foundation administered by the Israel Academy of Sciences and Humanities and by the fund for the promotion of research at the Technion.

Appendix A. Calculation of $\zeta(r,t)$

The 'modified' vorticity perturbation is governed by (3.10)–(3.12) which in principle are to be supplemented by specification of an initial distribution

$$\zeta(r,t) = \zeta_0(r) \quad \text{at} \quad t = 0. \tag{A 1}$$

The solution of this linear initial- and boundary-value problem may be represented as the superposition of the solutions respectively corresponding to the above problem with a homogeneous initial condition and with a homogeneous boundary condition at $r = 1$. The latter contributes to the evolution equation a decaying forcing term which is independent of both $\gamma(t)$ and $\eta(t)$ (cf. Frankel & Weihs 1987) and is therefore omitted†, i.e. we select $\zeta_0(r) = 0$ in (A 1). We thus obtain

$$\zeta(r,t) = -2k \sum_{n=1}^{\infty} \frac{\alpha_n r J_1(\alpha_n r)}{J_0(\alpha_n)} \times \int_0^t \left[\left(\frac{\partial \sigma}{\partial \Gamma} \right)^{(0)} \gamma(\tau) - 2S \frac{\mathrm{d}\eta}{\mathrm{d}\tau} \right] \exp[-S(k^2 + \alpha_n^2)(t-\tau)] \, \mathrm{d}\tau. \tag{A 2}$$

† A similar question arises in the context of formulating the problem governing $c_0(x,t)$. Thus, the replacement of (3.22c) by a non-homogeneous initial condition results likewise in the introduction of a decaying forcing term into (3.28).

This in conjunction with the relation

$$\int_0^1 rI_1(kr)J_1(\alpha_n r)\,\mathrm{d}r = -\left(k^2+\alpha_n^2\right)^{-1}\alpha_n I_1(k)J_0(\alpha_n) \tag{A 3}$$

yields (3.15).

The limit $S \ll 1$:

We consider the case $\epsilon \ll S \ll 1$ (cf. Appendix B) for $k \sim O(1)$. (A similar calculation may be carried out to obtain ζ for larger values of k.) In the 'outer' limit $S \to 0$ when $1-r \sim O(1)$, ζ vanishes. Define the inner variable $1-r = S^{1/2}y$ to obtain from (3.10)

$$\frac{\partial\zeta}{\partial t} \sim \frac{\partial^2\zeta}{\partial y^2} + S^{1/2}\frac{\partial\zeta}{\partial y} + O(S), \tag{A 4}$$

which is supplemented by (3.12) and homogeneous initial (at $t = 0$) and matching (for $y \to \infty$) conditions. Substituting the expansion

$$\zeta(y,t) \sim \zeta_0(y,t) + S^{1/2}\zeta_1(y,t) + O(S),$$

we obtain

$$\zeta_0(y,t) = \frac{ky}{2\pi^{1/2}}\int_0^t \left[\frac{1}{S}\left(\frac{\partial\sigma}{\partial\Gamma}\right)^{(0)}\gamma - 2\frac{\mathrm{d}\eta}{\mathrm{d}\tau}\right](t-\tau)^{-3/2}\exp\left[-\frac{y^2}{4(t-\tau)}\right]\mathrm{d}\tau, \tag{A 5a}$$

$$\zeta_1(y,t) = \int_0^t\int_0^\infty G(y,t,y_0,t_0)\frac{\partial\zeta_0}{\partial y_0}\,\mathrm{d}y_0\,\mathrm{d}t_0, \tag{A 5b}$$

wherein $G(y,t,y_0,t_0)$ is that appearing in (3.24*b*). Expanding $I_1(kr)$ into a Taylor series in powers of y, substituting (A 5) and (3.24*b*) and neglecting exponentially small terms, we obtain (3.16).

Appendix B. Kinetic data

In the following we estimate the order of magnitude of the requisite kinetic parameters for a water jet of radius $a = 0.1$ cm moving in air at atmospheric pressure and room temperature (25 °C). From their respective definitions, making use of the values of the density and viscosity of water and the surface tension of clean water in air, we readily obtain for the capillary time scale $T_c \approx 3.7\times10^{-3}$ s (and the parameter $S \approx 3.7\times10^{-3}$). Considering effects of solute mass transfer on jet stability, we focus on the lower-molecular-weight alcohols which are significantly volatile and soluble in water. A thorough tabulation of diffusion coefficients of organic compounds in aqueous solutions (Johnson & Babb 1956) shows only a moderate spread of the data for the diffusion coefficients of the lower alcohols about $D \approx 10^{-5}\,\mathrm{cm^2\,s^{-1}}$. (The accurate numerical value of D is of minor importance since throughout the derivation the various parameters only involve $D^{1/2}$.) We thus indeed have $\epsilon \ll 1$. Furthermore $S/\epsilon = \mu/\rho D$, i.e. the Schmidt number $\approx 10^3$ (cf. the comments preceding (3.26)). Following the standard practice (Hansen 1960; Crank 1975), solute mass transfer within the surrounding atmosphere is modelled by use of the mass-transfer coefficient E in (2.4) and (2.5*b*). We estimate this coefficient via the penetration approximation (cf. Bird, Stewart & Lightfoot 1960; Sherwood, Pigford & Wilke 1975) $E \approx (D_g/T)^{1/2}$. For the above-mentioned organic compounds the diffusivity in air is (Lugg 1968)

$D_g \approx 0.1\,\mathrm{cm^2\,s^{-1}}$. Taking as an average representative value $T \approx 10T_c$ one obtains $E \approx 1.5\,\mathrm{cm\,s^{-1}}$.

Explicit results are presented in § 4 for a system satisfying the Langmuir–Hinshelwood kinetic relation (4.1) which at equilibrium reduces to the Langmuir isotherm. Neglecting interaction phenomena (such as 'cooperative adsorption'), the latter is the simplest nonlinear isotherm which is widely used when significant surface-tension variations occur (Chang & Franses 1995; Eastoe & Dalton 2000). Lin, McKeigue & Maldarelli (1991) present experimental evidence that interaction phenomena only become significant for octanol, hence adsorption of lower alcohols can adequately be described by the Langmuir isotherm. Kinetic parameters characterizing this isotherm obtained via analysis of surface-tension relaxation experiments are tabulated by Chang & Franses (1995), Dukhin, Kretzschmar & Miller (1995) among others. The data regarding Γ_m, the saturation surface-excess concentration, show a small scatter for the lower alcohols and no definite trend in the variation with molecular weight, $\Gamma_m \approx (6\text{–}9)\times 10^{-10}\,\mathrm{mole\,cm^{-2}}$. Given that Γ_m is nearly constant for the various solutes, their respective surface activities are essentially determined by β_l which increases by an approximately constant factor of 3–4 (cf. Hommelen 1959; Chang & Franses 1995) with the addition of each CH_2 group to the solute molecular chain. Data regarding K_l, the adsorption-rate constant, are provided by Joos & Serrien (1989) for the normal alcohols (from propanol to heptanol).

Results of the present stability analysis are illustrated making use of the intermediate values $\Gamma_m \approx 7\times 10^{-10}\,\mathrm{mole\,cm^{-2}}$, $\beta_l = 2.1\times 10^5\,\mathrm{cm^3\,mole^{-1}}$ and $K_l = 1.6\times 10^{-2}\,\mathrm{cm\,s^{-1}}$ appropriate to the approximate description of the hexanol–water–air system. Making use of Henry's law constant for this system at 25 °C (Yaws 1999) and assuming ideal behaviour of the gaseous phase, we obtain the partition coefficient $K_p \approx 8.6\times 10^{-4}$. From the solubility of hexanol in water at 25 °C (Yaws 1999) together with the value of K_p we obtain the saturation value of $C_\infty \approx 5.0\times 10^{-8}\,\mathrm{mole\,cm^{-3}}$.

At equilibrium the subsurface concentration for a given $\Gamma^{(0)}$ is inversely proportional to the value of the parameter β. Thus, once K_p, the partition coefficient, has been determined, β_g (pertaining to adsorption from the surrounding atmosphere) is readily obtained as $\beta_g = \beta_l/K_p$. The value of the rate constant K_g is estimated by means of Eyring's theory of absolute reaction rates. According to this theory (cf. Glasstone, Laidler & Eyring 1941; Joos 1995), the rate constants K_i $(i = l, g)$ are proportional to the equilibrium constant between the activated complex and the reactants (i.e. solute molecules within the substrate and active sites on the adsorbing interface). Accordingly, $K_g/K_l = K_p^{-1}$.

REFERENCES

Anshus, B. E. 1973 The effect of surfactants on the breakup of cylinders and jets. *J. Colloid Interface Sci.* **43**, 113–121.

Berger, S. A. 1988 Initial-value stability analysis of a liquid jet. *SIAM J. Appl. Maths* **48**, 973–991.

Bird, R. B., Stewart, W. E. & Lightfoot, E. N. 1960 *Transport Phenomena.* Wiley.

Borwankar, R. P. & Wasan, D. T. 1983 The kinetics of adsorption of surface-active agents at gas-liquid interfaces. *Chem. Engng Sci.* **38**, 1637–1649.

Burkholder, H. C. & Berg, J. C. 1974 Effect of mass transfer on laminar jet breakup: part I. Liquid jets in gases. *AIChE J.* **20**, 863–872.

Chandrasekhar, S. 1961 *Hydrodynamic and Hydromagnetic Stability*. Oxford University Press.

Chang, C. H. & Franses, E. I. 1995 Adsorption dynamics of surfactants at the air/water interface; a critical review of mathematical models, data, and mechanisms. *Colloids Surfaces* A **100**, 1–45.

Coyle, R. W., Berg, J. C. & Niwa, J. C. 1981 Liquid–liquid jet breakup under conditions of relative motion, mass transfer and solute adsorption. *Chem. Engng Sci.* **36**, 19–28.

Crank, J. 1975 *The Mathematics of Diffusion*. Clarendon.

Dukhin, S. S., Kretzschmar, G. & Miller, R. 1995 Dynamics of adsorption at liquid interfaces: Theory, experiment, application. In *Studies in Interface Science* (ed. D. Möbius & R. Miller). Elsevier.

Eastoe, J. & Dalton, J. S. 2000 Dynamic surface tension and adsorption mechanisms of surfactants at the air–water interface. *Adv. Colloid Interface Sci.* **85**, 103–144.

Edwards, D. A., Brenner, H. & Wasan, D. T. 1991 *Interfacial Transport Processes and Rheology*. Butterworths-Heinemann.

Frankel, I. & Weihs, D. 1987 Influence of viscosity on the capillary instability of a stretching jet. *J. Fluid Mech.* **185**, 361–383.

Glasstone, S., Laidler, K. J. & Eyring, H. 1941 *The Theory of Rate Processes*. McGraw-Hill.

Hansen, R. S. 1960 The theory of diffusion controlled absorption kinetics with accompanying evaporation. *J. Phys. Chem.* **64**, 637–641.

Hommelen, J. R. 1959 The elimination of errors due to evaporation of the solute in the determination of surface tensions. *J. Colloid Sci.* **14**, 385–400.

Johnson, P. A. & Babb, A. L. 1956 Liquid diffusion in non-electrolytes. *Chem. Rev.* **56**, 387–453.

Joos, P. 1995 Kinetic equations for transfer-controlled adsorption kinetics. *J. Colloid Interface Sci.* **171**, 399–405.

Joos, P. & Serrien, G. 1989 Adsorption kinetics of lower alkanols at the air/water interface: Effect of structure makers and structure breakers. *J. Colloid Interface Sci.* **127**, 97–103.

Lin, S. Y., McKeigue, K. & Maldarelli, C. 1991 Diffusion-limited interpretation of the induction period in the relaxation in surface tension due to the adsorption of straight chain, small polar group surfactants: Theory and experiment. *Langmuir* **7**, 1055–1066.

Lugg, G. A. 1968 Diffusion coefficients of some organic and other vapours in air. *Anal. Chem.* **40**, 1072–1077.

MacLeod, C. A. & Radke, C. J. 1994 Surfactant exchange kinetics at the air/water interface: Dynamic tension of growing liquid drops. *J. Colloid Interface* **166**, 73–88.

Pearson, J. R. A. 1958 On convection cells induced by surface tension. *J. Fluid Mech.* **4**, 489–500.

Prosperetti, A. 1977 Viscous effects on perturbed spherical flows. *Q. Appl. Maths* **34**, 339–352.

Rayleigh, Lord 1878 On the instability of jets. *Proc. Lond. Math. Soc.* **10**, 4–13.

Scriven, L. E. & Sternling, C. V. 1964 On cellular convection driven by surface-tension gradients: Effects of mean surface tension and surface viscosity. *J. Fluid Mech.* **19**, 321–340.

Sherwood, T. K., Pigford, R. L. & Wilke, C. R. 1975 *Mass Transfer*. McGraw-Hill.

Skelland, A. H. P. & Walker, P. G. 1989 Effects of surface active agents on jet breakup in liquid-liquid systems. *Can. J. Chem. Engng* **67**, 762–770.

Sternling, C. V. & Scriven, L. E. 1959 Interfacial turbulence: Hydrodynamic instability and the Marangoni effect. *AIChE J.* **5**, 514–523.

Tarr, L. E. & Berg, J. C. 1980 The effect of nonlinear concentration profiles on the breakup of jets undergoing mass transfer. *Chem. Engng Sci.* **35**, 1465–1467.

Yaws, C. L. 1999 *Chemical Properties Handbook. Physical, Thermodynamical, Environmental, Transport, Safety, and Health Related Properties for Organic and Inorganic Chemicals*. McGraw-Hill.